Metal-insulator-superconductor transition of spin-3/2 atoms on optical lattices

Theja N. De Silva

Phys. Rev. A **97**, 013632 — Published 29 January 2018

DOI: 10.1103/PhysRevA.97.013632

Metal-Insulator-Superconductor transition of spin-3/2 atoms on optical lattices

Theja N. De Silva
Department of Chemistry and Physics, Augusta University, Augusta, GA 30912, USA.
Kavli Institute for Theoretical Physics, University of California, Santa Barbara, CA 93106, USA.
Institute for Theoretical Atomic, Molecular, and Optical Physics,
Harvard-Smithsonian Center for Astrophysics, Harvard University, Cambridge, MA 02138, USA.

We use a slave-rotor approach within a mean-field theory to study the competition of metallic, Mott-insulating, and superconducting phases of spin-3/2 fermions subjected to a periodic optical lattice potential. In addition to the metal, the Mott-insulator, and the superconducting phase that associates with the gauge symmetry breaking of spinon field, we identify a novel emerging superconducting phase that breaks both roton and spinon field gauge symmetries. This novel superconducting phase emerges as a result of the competition between spin-0 singlet and spin-2 quintet interaction channels naturally available for spin-3/2 systems. The two superconducting phases can be distinguished from each other from quasiparticle weight. We further discuss the properties of these phases for both two-dimensional square and three-dimensional cubic lattices at zero and finite temperatures.

I. I. INTRODUCTION

Recent extraordinary progress achieved in trapping and manipulating of ultra-cold atomic gases provides a wonderful opportunity for exploring quantum many-body physics. Ultra-cold atomic systems are now considered as one of the most promising and efficient playgrounds for studying condensed matter and nuclear physics phenomena [1]. Recent developments in laser technology and experimental advancements allow one to have unprecedented control over various experimental parameters [2]. Effective spatial dimensionality, lattice structure, and lattice geometry can be tuned by adjusting the laser intensity, phase, and wavelength. The interaction between the atoms can be controlled dramatically by adjusting the two-body scattering length through magnetically tuned Feshbach resonance. Through the first generation of experiments with ultra-cold bosons and fermions in optical lattices, it has been well-established that these systems can exhibit a variety of interesting phenomena [3–8]. The growing availability of multi-component degenerate fermionic atoms, such as ^{6}Li [9–11], ^{40}K [12], ^{135}Ba and ^{137}Ba [13], and ^{173}Yb [14] provides a controllable platform to study higher spin, strongly correlated physics that features novel phenomena.

Among multi-component ultra-cold gases, high spin fermions such as spin- 3/2 ^{132}Cs, ^{9}Ba, ^{135}Ba, and ^{201}Hg attracted much attention due to the rich collective phenomena they can exhibit [15–26]. Spin-3/2 systems are expected to show emerging behaviour due to the competing parameters, such as *total* spin-0 singlet and spin-2 quintet scattering lengths. The *total* spin-1 and spin-3 channels are prohibited due to the Pauli exclusion principle. In addition, the strong quantum fluctuations due to the enlarged SO(5) or Sp(4) symmetry is expected to play a bigger role in these systems [27, 28]. In particular, when these spin-3/2 atoms are subjected to a periodic lattice potential, they can show novel collective behaviour that are not obvious in spin-1/2 electronic systems. For example, on-site four-particle clustering instabilities can leads to quintet Cooper pairing favored by the spin-2 interaction channel [29–34]. When the total spin-0 interaction channel is strongly positive, the system can leads to a Mott-insulating state with a fixed number of atoms on each lattice site. It is the purpose of this paper to study the competition and phase transitions among metal, Mott-insulating, and singlet Cooper pairing states of neutral spin-3/2 fermions subjected to two-dimensional square lattice and three-dimensional cubic lattice. In order to do so, we use a slave rotor approach that allows us to handle the intermediate coupling regime where the charge fluctuations are strong [35]. In the slave-rotor representation, the particle operator is decomposed into a roton-bosonic field and a spinon-fermionic field. While the roton caries the charge degrees of freedom, the spinon caries the spin degrees of freedom. In this approach, the metal and Mott-insulating phases are characterized by breaking of global U(1) gauge symmetry associates with the charge degrees of freedom. In general superconducting phase is characterised by breaking of global U(1) symmetry associates with the spinon degrees of freedom.

In addition to the obvious metal, Mott-insulator, and conventional (in the sense that one gauge symmetry is broken) superconducting phases arising from the competing interactions, we find a novel emerging superconducting phase where both global symmetries associate with charge and spin degrees of freedom are broken. This novel superconducting phase is differentiated from the conventional superconducting phase due to the non-zero quasi particle weight. Notice that we use the condensed matter terminology, but our metal and superconducting phases are neutral for atoms in optical lattices. Further, we investigate each of these emerging phases at both zero temperature and finite temperature by calculating various physical quantities.

The paper is organized as follows. In section II, we introduce spin-3/2 model Hamiltonian for atoms on optical lattice. The model is a generalized Hubbard model

based on microscopic s-wave atom-atom interaction. In section III, we introduce the slave rotor approach and convert our model Hamiltonian in to a coupled rotor-spinon Hamiltonian. In section IV, a decoupling scheme is introduced to decouple the rotor part and the spinon part of the Hamiltonian. In section V and VI, we use a mean-field treatment to solve the rotor and spinon sectors of the Hamiltonian. In section VII and VIII, we discuss our zero temperature and finite temperature formalism and their results. Finally in section IX, we summarize our results with a discussion.

II. II. MODEL HAMILTONIAN

We start with the generic from of the spin-3/2 neutral particle Hamiltonian of the lattice model [27],

$$H = -t\sum_{\langle ij\rangle}(c^\dagger_{i\sigma}c_{j\sigma} + h.c) - \mu\sum_{i\sigma} c^\dagger_{i\sigma}c_{i\sigma}$$
$$+U_0\sum_i P^\dagger_{00}(i)P_{00}(i) + U_2\sum_{i,m=\pm2,\pm1,0} P^\dagger_{2m}(i)P_{2m}(i), \quad (1)$$

where $P^\dagger_{Fm}(i) = \sum_{\alpha\beta}\langle F,m|\alpha,\beta\rangle c^\dagger_{i\alpha}c^\dagger_{i\beta}$ are the singlet ($F=0$, $m=0$) and quintet ($F=2$, m) pairing operators and $c^\dagger_{i,\sigma}$ is the fermionic creation operator at site i, in one of the hyperfine spin state $\sigma = \pm1/2, \pm3/2$. Here,

$$U_s = \int d\vec{r}d\vec{r'}w^*(\vec{r}-\vec{R}_i)w^*(\vec{r'}-\vec{R}_i) \quad (2)$$
$$\times g_s w(\vec{r'}-\vec{R}_i)w(\vec{r}-\vec{R}_i),$$

is the interaction parameter for the total spin $S=0$ and $S=2$ channels with the contact interaction in free space $g_s = 4\pi\hbar^2 a_s/m$ and localized Wannier functions $w(\vec{r}-\vec{R}_i)$ at $\vec{R}_i$, where a_s is the s-wave scattering length for total spin-S channel. At half filling (ie, on average one atom per site), the particle-hole symmetry ensures the chemical potential $\mu = (U_0+5U_2)/4$ [27]. Here we assume that the atoms can hop between nearest-neighbors with hopping amplitude t, where $\langle ij\rangle$ stands for sum over only nearest neighbors.

For the purpose of studying the phase transition of metallic, insulating, and superconducting phases, it is convenient if we re-write the Hamiltonian in terms of spin-3/2 on-site singlet operator $P^\dagger_i \equiv P^\dagger_{00}(i) = 1/\sqrt{2}(c^\dagger_{i,3/2}c^\dagger_{i,-3/2} - c^\dagger_{i,1/2}c^\dagger_{i,-1/2})$ and the on-site density operator $n_i = \sum_\sigma c^\dagger_{i\sigma}c_{i\sigma}$ [36],

$$H = -t\sum_{\langle ij\rangle}(c^\dagger_{i\sigma}c_{j\sigma} + h.c) - \mu_0\sum_{i\sigma} c^\dagger_{i\sigma}c_{i\sigma}$$
$$+U/2\sum_i(\sum_\sigma c^\dagger_{i\sigma}c_{i\sigma} - 4/2)^2 + V\sum_i P^\dagger_i P_i \quad (3)$$

Here $U = 2U_2$ and $V = U_0 - U_2$ with the shifted chemical potential μ_0 is given by $(U_0-U_2)/4$ at half filling. This model has an exact SO(5) symmetry which reduces to a SU(4) symmetry at $U_0 = U_2$ [27, 37]. Notice that at this SU(4) symmetric limit, the chemical potential at half filling reaches to zero. Each major terms in the model competes for metallic, Mott-insulating, and singlet pairing states. At SU(4) limit and the interactions are weak compared to the tunneling energy, $U \ll t$, atoms can gain kinetic energy by hopping through the lattice. In the opposite limit where $U \gg t$, the repulsion is greater than the gain in kinetic energy, thus the atoms will localize at lattice sites, resulting a Mott-insulator. For $V < 0$, the model naturally favors the singlet pairing state while first two terms compete for metallic and Mott-insulating states, respectively. In addition to the singlet pairing, as discussed in Ref. [38], multi-particle clustering of spin-3/2 atoms can lead to quintet pairing states with total spin-2. The quintet pairing requires negative quintet interaction parameter U_2. Here we consider positive U_2 that supports Mott-insulating states, therefore we can safely neglect the possible quintet pairing in the model.

For deep optical lattices, one can approximate the Wannier functions by the Gaussian ground state in the local oscillator potential and find tunneling amplitude $t \propto E_r V_r^{3/4} e^{-2\sqrt{V_r}}$ is exponentially sensitive to laser intensity $V_0 = E_r V_r$ that used to create the optical lattice, here E_r is the recoil energy [39]. The interaction terms $U_s \propto a_s E_r V_r^{3/4}$ is linearly sensitive to scattering lengths and relatively, weakly sensitive to the laser intensity. As a result, the model is highly tunable in experimental setups in optical lattice environments.

III. III. SLAVE-ROTOR APPROACH

Slave-particle approaches are proven to be simple and computationally inexpensive approaches to study strongly correlated effects in many-particle systems and these approaches are capable of accounting for particle correlations beyond standard mean-field theories. The first slave-particle approach has been proposed to study the Mott insulator-metal transitions [40]. There are several advantages of using slave-particle approaches over other mean-field theories and the variational methods. While most variational approaches are valid only at zero temperature, the slave-particle approaches are applicable at both zero and finite temperatures. Unlike other mean-field theories, quantum fluctuations can be taken into account by Stratonovich-Hubbard transformation within the slave particle formalism [41]. Further, it has been shown that slave-particle approaches are equivalent to a statistically-consistent Gutzwiller approximation [42–44]. Here we use the slave-rotor approach as it is convenient for many component systems [35]. The method is simply introducing auxiliary boson to represent local degrees of freedom in the correlated system. The metallic solution will be described as a correlated Fermi liquid. In the

slave-rotor approach, the original local Fock space of the problem is mapped onto a larger local Fock space that contains as many fermions degrees of freedom as the original one and same number of spin-3/2 local quantum variables, one for each fermions. While new pseudo-fermion variable describes the itinerant quasiparticle fraction of the atom, the auxiliary boson describes its localized fraction.

The slave-rotor approach is first introduced by Florens and Georges for the Hubbard model to study metal-Mott insulator transition [35]. Later this approach has been applied to magnetic systems to study spin liquid phases [45–50]. In this approach, the particle operator is decoupled into a fermion and a bosonic rotor that carries the spin and the charge degrees of freedom, respectively. First, the particle operator $c_{i\sigma}$ that annihilate an atom with spin σ at site i is expressed as a product:

$$c_{i\sigma} = e^{-i\theta_i} f_{i\sigma}, \tag{4}$$

where the auxiliary fermion $f_{i\sigma}$ annihilates a spinon with spin σ and the local phase degree of freedom θ_i conjugates to the total (neutral) charge through the "angular momentum" operator $L_i = -i\partial/\partial\theta_i$,

$$[\theta_i, L_j] = i\delta_{ij}. \tag{5}$$

In this representation, while the rotor operator $e^{-i\theta_i}$ reduces the site occupation by one unit, the eigenvalues of the L_i correspond to the possible number of atoms on the lattice site. Notice that the name "angular momentum" is given due to the conservation of $O(2)$ variable $\theta_i \in [0, 2\pi]$ but nothing to do with physical angular momentum of the atoms. Using the fact that rotons and spinons commute, one can show that the number operator of the physical particles coincide with that of spinon;

$$n_{i\sigma} = c^\dagger_{i\sigma} c_{i\sigma} = f^\dagger_{i\sigma} f_{i\sigma} = n^f_{i\sigma}. \tag{6}$$

As the eigenvalues of the angular momentum operator $l \in Z$ can have any integer values, one must impose a constraint to truncate the enlarge Hilbert space to remove unphysical states,

$$L_i = \sum_\sigma n^f_{i\sigma} - 1. \tag{7}$$

This constraint glues charge and spin degrees of freedom and can be taken into account by introducing a Lagrange multiplier in the formalism. Notice that the angular momentum operator L_i measure the particle number at each site relative to the half-filling. In terms of new variables, our Hamiltonian in Eq. (3) becomes,

$$H = -t\sum_{\langle ij\rangle} f^\dagger_{i\sigma} f_{j\sigma} e^{i(\theta_i-\theta_j)} - (\mu_0 + h)\sum_{i\sigma} f^\dagger_{i\sigma} f_{i\sigma} + \frac{U}{2}\sum_i L_i^2 + +V\sum_i P_i^\dagger P_i, \tag{8}$$

where pairing operators in the last term now has the form $P_i^\dagger = 1/\sqrt{2}(f^\dagger_{i,3/2} f^\dagger_{i,-3/2} - f^\dagger_{i,1/2} f^\dagger_{i,-1/2}) e^{2i\theta_i}$. Notice that the constraint is treated on average so that Lagrange multiplier h is site independent. Even though one interaction term in $S = 2$ channel simply becomes the kinetic energy for the rotons, the pairing interaction term is still quartic and the hopping term now becomes quartic in spinon and rotor operators as well. In the following section, we make further approximations to the quartic terms to get a manageable theory.

IV. IV. DECOUPLING SPINON AND ROTORS

For spin-3/2 atoms on square or cubic lattices at half filling, we plan to decouple the Hamiltonian in Eq. (8) by using a mean field description. First, we decouple the hopping term so that the Hamiltonian H becomes the sum of independent spinon and rotor parts: $H \to H_f + H_\theta$. This will lead to H_θ part to be an interacting quantum XY model and H_f part to be an interacting f-particle spinon part. We will then make a second mean-field treatment to each part of the Hamiltonian to convert them into effectively non-interacting ones. At half-filling, particle-hole symmetry requires Lagrange multiplier $h = 0$ and $\mu_0 = (U_0 - U_2)/4$. We introduce three mean-fields as follows;

$$\Delta = \frac{|V|}{2}\langle f^\dagger_{i,3/2} f^\dagger_{i,-3/2} - f^\dagger_{i,1/2} f^\dagger_{i,-1/2}\rangle_f \tag{9}$$

$$Q_\theta = \sum_\sigma \langle f^\dagger_{i\sigma} f_{j\sigma}\rangle_f \tag{10}$$

$$Q_f = \langle e^{i(\theta_i-\theta_j)}\rangle_\theta \tag{11}$$

where i and j are nearest-neighbor sites. The subscript f or θ means that the quantum and thermal expectation values must be taken with respect to the spinon and roton sectors, respectively. Here we make the assumptions that these expectation values are real and independent of bond directions. One can relax these assumptions and treat orbital current around a plaquette. After performing the decoupling scheme, the spinon and rotor part of the Hamiltonian becomes,

$$H_f = -tQ_f \sum_{\langle ij\rangle,\sigma} (f^\dagger_{i\sigma} f_{j\sigma} + h.c) - \mu_0 \sum_{i\sigma} f^\dagger_{i\sigma} f_{i\sigma} + \Delta\sum_i (f^\dagger_{i,3/2} f^\dagger_{i,-3/2} - f^\dagger_{i,1/2} f^\dagger_{i,-1/2} + h.c) \tag{12}$$

$$H_\theta = -tQ_\theta \sum_{\langle ij\rangle} (X_i^\dagger X_j + h.c) - \lambda\sum_i X_i^\dagger X_i - \frac{1}{2U}\sum_i (i\partial_\tau X_i^\dagger)(-i\partial_\tau X_i), \tag{13}$$

where $X_i = e^{i\theta_i}$ and λ is the Lagrange multiplier to impose the condition $|X_i|^2 = 1$. At the operator level, the Hamiltonian is now decoupled and while the spinon part is quadratic, the rotor part is naturally interacting. While mean field parameter Q_f renormalizes the hopping term and related to the effective mass $m^* = mQ_f$, the expectation value of pairing operator, Δ represents the pairing of spinons.

V. V. MEAN-FIELD TREATMENT TO SPINON PART

The spinon part can easily be diagonalized in the momentum space. Performing Fourier transform into momentum space and then usual Bogoliubov transformation, the spinon Hamiltonian has the form,

$$H_f = \sum_{k,l} \Lambda_l(k)\eta^\dagger_{k,l}\eta_{k,l} + \frac{1}{2}\sum_{k,l}[A^l_{kk} - \Lambda_l(k)], \qquad (14)$$

where $\eta_{k,l}$ is a four component vector representing quasi-spinons and $\Lambda_l(k) = \pm\sqrt{\epsilon_k^2 + \Delta^2}$ (twice) are the eigenvalues with $l = 1, 2, 3, 4$. Here $A^l_{kk'}$ is 4×4 diagonal matrix with diagonal element $\epsilon_k = -Q_f\gamma_k - \mu_0$, where $\gamma_k = 2t\sum_\alpha \cos k_\alpha$ with $\alpha = x, y, z$ and here the lattice momentum is re-scaled with the lattice constant. The quantum and thermal expectation value of the Eq. (9) with respect to the Hamiltonian H_f leads to the gap equation,

$$\frac{4}{V} = -\frac{1}{N_s}\sum_k \frac{\tanh(\beta E_k/2)}{E_k}, \qquad (15)$$

where $E_k = \sqrt{\epsilon_k^2 + \Delta^2}$ with the total number of lattice sites N_s and dimensionless inverse temperature β. Summing over nearest-neighbors and then calculating the expectation value in Eq. (10) with respect to H_f gives,

$$\eta t Q_\theta = \frac{1}{N_s}\sum_{k,\sigma} \gamma_k n_k \qquad (16)$$

where η is the number of nearest neighbors and the average occupation n_k is given by,

$$n_k = \frac{1}{2} - \frac{\epsilon_k}{2E_k}\tanh(\beta E_k/2). \qquad (17)$$

The two self-consistent equations derived in Eq. (15) and Eq. (16) must be solved with the Eq. (11) which can be written as $Q_f = \langle X_i^\dagger X_j\rangle_\theta$.

VI. VI. MEAN-FIELD TREATMENT TO ROTON PART

The calculation of Q_f requires a special attention as X bosons can undergo Bose-Einstein condensation. The metallic (or band-insulating) phase corresponding to the ordering of rotors, and thus spontaneously break the $O(2)$ symmetry. The rotor disordered phase corresponds to the Mott-insulating phase given that the system is non-superfluid. Notice the metal to Mott-insulator transition is driven by spontaneous global $U(1)$ symmetry associates with the charge degrees of freedom. However, the Mott transition emerging from the slave rotor approach does not break any spin rotational symmetry, thus the transition is into a non-magnetic phase.

The final self-consistent equation can easily be calculated using functional integral approach to the roton part of the Hamiltonian with the constraint equation $|X_i|^2 = 1$. Introducing the rotor Green's function $G_\theta(k, \tau) = \langle X_k(\tau)X_k^\dagger(0)\rangle$, the constraint equation becomes,

$$\frac{1}{N_s}\sum_k \frac{1}{\beta}\sum_n G_\theta(k, i\nu_n) = 1, \qquad (18)$$

where $\nu_n = 2n\pi/\beta$ are the bosonic Matsubara frequencies. In coherent state path integral representation, the rotor Green's can be written as,

$$G_\theta(k, \tau) = \frac{\int\prod_{ki}\frac{dX_{ki}dX^*_{ki}}{2\pi i}X(\tau)X^*_k(0)e^{-S_\theta}}{\int\prod_{ki}\frac{dX_{ki}dX^*_{ki}}{2\pi i}e^{-S_\theta}}, \qquad (19)$$

where time index i labeling runs from 0 to ∞ corresponding to $\tau = 0$ and $\tau = \beta$, respectively. The action in the momentum space associates with the rotor part of the Hamiltonian is given by,

$$S_\theta = \int_0^\beta d\tau \sum_k X^*_k(-\frac{1}{2U}\partial^2_\tau - \lambda - Q_\theta\gamma_k)X_k. \qquad (20)$$

Following the standard path integral formalism, the rotor Green's function for the non-zero wave vector is given by,

$$G_\theta(k, i\nu_n) = [\nu_n^2/U + \lambda - Q_\theta\gamma_k]^{-1}. \qquad (21)$$

Notice that following the Ref. [35], a renormalization of $U \to U/2$ has been performed to preserve the exact atomic limit. Then writing,

$$\frac{1}{\beta}\sum_n G_\theta(k, i\nu_n) = \frac{U}{\beta}\sum_n \frac{1}{i\nu_n + \sqrt{U(\lambda - Q_\theta\gamma_k)}} \times\frac{1}{-i\nu_n + \sqrt{U(\lambda - Q_\theta\gamma_k)}}, \qquad (22)$$

performing a suitable contour integration, we find

$$\frac{1}{\beta}\sum_n G_\theta(k,i\nu_n) = \frac{U}{2\sqrt{U(\lambda - Q_\theta\gamma_k)}} \coth[\frac{\beta}{2}\sqrt{U(\lambda - Q_\theta\gamma_k)}]. \quad (23)$$

Combining this with Eq. (18) and separating $k = 0$ term leads the constraint equation to be,

$$1 = Z + \frac{1}{2N_s}\sum_{k\neq 0}\sqrt{\frac{U}{\lambda - Q_\theta\gamma_k}} \times \coth[\frac{\beta}{2}\sqrt{U(\lambda - Q_\theta\gamma_k)}], \quad (24)$$

where $0 \leq Z \leq 1$ is the rotor condensate amplitude which represents the quasiparticle weight. As the rotor condensation indicates the transition into the metallic phase, non-zero quasiparticle weight Z represents the metallic state. In the non-interacting limit $Z \to 1$. Finally, summing over nearest-neighbors of Eq. (11) and transforming into Fourier space leads to

$$\eta t Q_f = \eta t Z + \frac{1}{N_s}\sum_{k\neq 0}\frac{\gamma_k}{\beta}\sum_n G_\theta(k,i\nu_n). \quad (25)$$

Completing the contour integration, our final self consistent equation becomes,

$$\eta t Q_f = \eta t Z - \frac{1}{2N_s}\sum_{k\neq 0}\gamma_k\sqrt{\frac{U}{\lambda - Q_\theta\gamma_k}} \times \coth[\frac{\beta}{2}\sqrt{U(\lambda - Q_\theta\gamma_k)}]. \quad (26)$$

This Q_f is the mass enhancement factor of the quasiparticle, thus it is proportional to the effective mass of the quasiparticle $m^* = Q_f m$, where m is the bare mass of the free atoms. As the second term in Eq. (26) is negative, mass enhancement is always greater than the quasiparticle weight, $Q_f > Z$ at the saddle point level, and remains finite even away from metallic phase where Z vanishes.

VII. VII. ZERO TEMPERATURE FORMALISM AND QUANTUM PHASE TRANSITIONS

For spin-3/2 atoms on a d-dimensional lattice at zero temperature, four self-consistent equations can be largely simplified. First, by introducing the d-dimensional density of states, $D(\epsilon) = \frac{1}{N_s}\int \frac{d^dk}{(2\pi)^d}\delta(\epsilon + \gamma_k)$ and setting energy units to be $t = 1$, our self consistent equations become,

$$\frac{4}{V} = -\int d\epsilon D(\epsilon)\frac{1}{\sqrt{(Q_f\epsilon - \mu_0)^2 + \Delta^2}}, \quad (27)$$

$$\eta Q_\theta = -\int d\epsilon D(\epsilon)\epsilon\left(\frac{1}{2} - \frac{Q_f\epsilon - \mu_0}{2\sqrt{(Q_f\epsilon - \mu_0)^2 + \Delta^2}}\right), \quad (28)$$

$$1 = Z + \frac{1}{2}\int d\epsilon D(\epsilon)\sqrt{\frac{U}{\lambda + Q_\theta\epsilon}}, \quad (29)$$

and,

$$\eta Q_f = \eta Z - \frac{1}{2}\int d\epsilon D(\epsilon)\epsilon\sqrt{\frac{U}{\lambda + Q_\theta\epsilon}}, \quad (30)$$

where the nearest-neighbor coordination number is η and these self-consistent equations are valid only at zero temperature for a half filled system whose chemical potential is given by $\mu_0 = (U_0 - U_2)/4$.

Obviously, the superconducting phase is characterized by the non-zero singlet pairing order parameter Δ. The gap equation gives non-zero solutions for the pairing order parameter for all $V < 0$, thus the superconducting transition line in $U_0 - U_2$ parameter space is given by the equation $U_0 = U_2$. This is the SU(4) symmetric line which can be alternatively represented by $\mu_0 = 0$. In the metallic phase rotors are condensed so that the non-zero value of the condensate amplitude or the quasiparticle weight Z signifies the metallic state. In the metallic phase, a macroscopic fraction of rotors occupy the lowest energy $E_l = -\eta t Q_\theta$ and the Lagrange multiplier or the rotor chemical potential $\lambda = -E_l \equiv \eta t Q_\theta$ remains constant. The quantum phase transition from the metallic state to Mott-insulating state is characterized by the vanishing quasiparticle weight Z. In the Mott-insulating phase the quasiparticle weight Z is zero and the rotor chemical potential $\lambda > \eta t Q_\theta$ needs to be determined by self consistently. The metal-insulator transition line can be determined by setting $\Delta = 0$, $Z = 0$, and $\lambda = \eta t Q_\theta$ in self-consistent equations presented above.

For a two-dimensional square lattice, the density of states can be approximated by a closed form using the elliptic integral of first kind K, $D(\epsilon) = \frac{1}{2\pi^2}K(1 - \epsilon^2/16)$ for $-4t \leq \epsilon \leq 4t$, and zero otherwise. Therefore for both metal and Mott-insulating phases, where $\Delta = 0$, Q_θ has an analytical form. Evaluating the integral in Eq. (28) for a two-dimensional square lattice, we find,

$$Q_\theta = \frac{1}{2\pi^2}K(1 - \mu_0^2/16)[16 - \mu_0^2]. \quad (31)$$

Notice that the chemical potential $\mu_0 = (U_0 - U_2)/4$ at half filling, thus Q_θ depends on the interaction parameters. This is in contrast with the regular Hubbard

model with spin-1/2 particles where $Q_\theta = 4/\pi^2$ is independent of the interaction [51]. Here at SU(4) limit where $\mu_0 = 0$, we find $Q_\theta = 8/\pi^2$ where extra factor 2 comes from the extra spin for the spin-3/2 system. For three-dimensional cubic lattice, we numerically evaluate Q_θ value. Re-arranging Eq. (30), we find a self-consistent equation for the critical U_2 value for the metal-insulator transition,

$$U_2^{CMI} = 16 Q_\theta^C \Big\{ \int \frac{d\epsilon D(\epsilon)}{\sqrt{1+\epsilon/4}} \Big\}^{-2}, \qquad (32)$$

where $Q_\theta^C = Q_\theta(U_2 = U_2^{CMI})$ depends on the critical interaction through the chemical potential.

Zero temperature phase diagrams for both square and cubic lattices in $U_0 - U_2$ plane are given in FIG. 1. There are four different phases at half filling, a metallic phase (M) at smaller value of $U_2 < U_0$, a Mott-insulating phase (MI) at larger values of $U_2 < U_0$, and two distinct superconducting phases (Z-SC and SC) for larger values of $U_2 > U_0$. In Z-SC phase quasiparticle weight Z is non-zero and it reaches to zero at the SC - Z-SC boundary breaking O(2) rotor symmetry. The boundary of Z-SC and SC phase is determined by solving our self-consistent equations with the conditions, $Z = 0$ and $\lambda = \eta t Q_\theta$. With our numerical calculations, we find Q_f remains constant along Z-SC-SC boundary, giving $Q_f \approx 0.255$ for two-dimensional square lattice and $Q_f \approx 0.104$ for three-dimensional cubic lattice. As to our knowledge, this new emergent Z-SC phase in which both U(1) symmetries associate with rotor degrees of freedom and spinon degrees of freedom are broken, has not been discussed before.

For two-dimensional square lattice, the quasiparticle weight Z, the mass enhancement Q_f, the average kinetic energy of the spinons Q_θ, and the pairing order parameter Δ are shown at fixed values of $U_0 = 6t$ and $U_0 = 2t$ in Fig. 2. As can be seen from the left panel of FIG 2, the quasiparticle weight is unity at non-interacting level of rotors, and then reaches to zero at the metal-insulator boundary. Meantime the superconducting order parameter picks a finite value at the insulator-superconductor boundary and increases as one increases the interaction parameter U_2 beyond U_0. Both quasiparticle weight and superconducting order parameter remain at zero at the intermediate Mott-insulating phase. The right panel of FIG 2 shows the variation of parameters across quantum phase transition from metal to Z-SC to SC phases. For a fixed value of $U_0 = 2t$, the metallic phase exists for low values of $U_2 \leq 2$ indicating non-zero quasiparticle weight Z and zero pairing order parameter Δ. For intermediate values of U_2, both quasi particle weight and pairing order parameter become non-zero, thus represents the Z-SC phase. As can be seen from the right panel in the SC phase, while quasiparticle weight vanishes, the pairing order parameter remains non-zero beyond $U_2 \approx 3.3t$. Notice, both mass enhancement and average kinetic energy of the rotons are non-zero across all quantum phase transitions, however Q_f shows small discontinuities at the quantum phase transitions. This zero-temperature discontinuity of mass enhancement factor Q_f is an artifact of the mean-field theory and it can be recovered by adding fluctuations over the mean fields, as we discussed in discussion section.

VIII. VIII. FINITE TEMPERATURE PHASE TRANSITIONS

For two-dimensional fermions on a lattice, the finite temperature phase transitions are absent, but one can expect to have crossovers. For three-dimensional fermions on a lattice, the finite temperature phase transitions are not forbidden. We numerically solve the finite temperature self consistent equations for the cubic lattice. As a demonstration, we show some finite temperature properties of the metallic phase and Z-SC phase in FIG. 3. The left panel shows the temperature dependence of the quasiparticle weight Z, the mass enhancement factor Q_f, and, the average kinetic energy Q_θ in the metallic phase where the interaction parameters are fixed to be $U_2 = 2t$ and $U_0 = 4t$. Unlike zero temperature metal-Mott insulator transition, the finite temperature metal-insulator phase transition is found to be of first order, thus Z shows a discontinuity at the transition. However, we find Q_f and Q_θ remain to be continuous at the transition. The right panel shows temperature dependence of the singlet pairing order parameter Δ, Q_f and Q_θ at the interaction parameters $U_2 = 1.5t$ and $U_0 = 0.5t$. The ground state at these interaction parameters is Z-SC phase where both singlet pairing order parameter Δ and quasiparticle weight Z are non-zero. The continuously vanishing singlet order parameter at a high temperature indicates the second order thermal transition from the Z-SC phase.

IX. IX. DISCUSSION AND CONCLUSIONS

As discussed above, all zero temperature quantum phase transitions are second order, however we find a discontinuity in mass enhancement factor Q_f when the transition is into Mott-insulating phase. On the other hand, while finite temperature thermal phase transition into the Mott-insulating phase is first order, we do not find any discontinuity in the mass enhancement factor. In our approach, the zero temperature Mott-transition is continuous, thus one expects continuous destruction of metallic Fermi surface. This would lead to a metal to have instabilities toward a magnetic Mott-insulator due to the Fermi surface nesting, though we have not considered any symmetry breaking insulating states in our approach.

The two superconducting phases discussed above are distinguished due to two main reasons. In the Z-SC phase, both rotor and pair of spinons are in condensate. As a result, the broken U(1) gauge symmetry in the rotor sector gives non-zero quasiparticle weight as similar

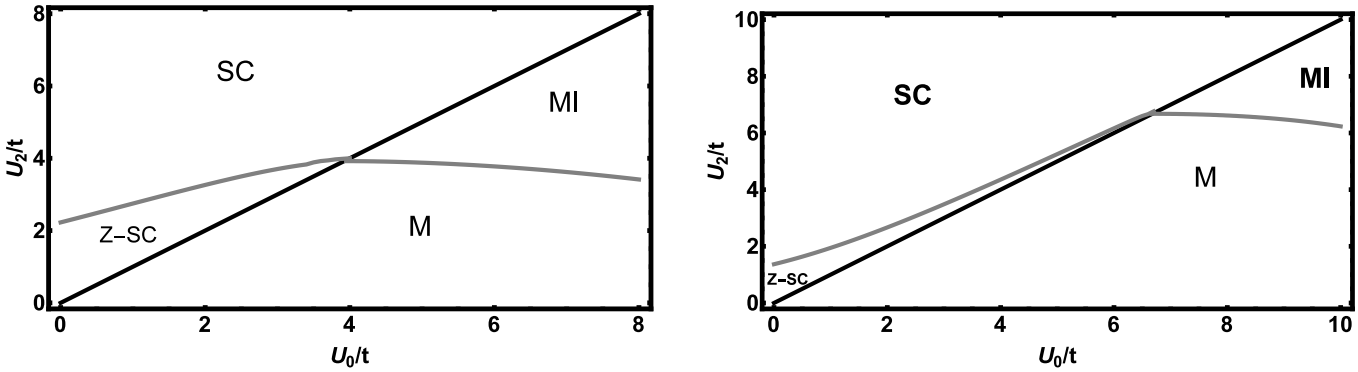

FIG. 1: Zero temperature phase diagram showing four different phases; M: metallic phase, MI: Mott-insulating phase, Z-SC: superconducting phase with non-zero quasiparticle weight, and SC: superconducting phase with zero quasiparticle weight. Left: The phase diagram for two-dimensional square lattice. Right: The phase diagram for three-dimensional cubic lattice. The metal phase is characterized by global U(1) symmetry broken state associates with the rotor degrees of freedom and both superconducting phases (SC and Z-SC) are characterized by the global U(1) symmetry broken states associates with the spinon degrees of freedom. The Z-SC phase shows additional U(1) symmetry breaking associates with the rotor sector.

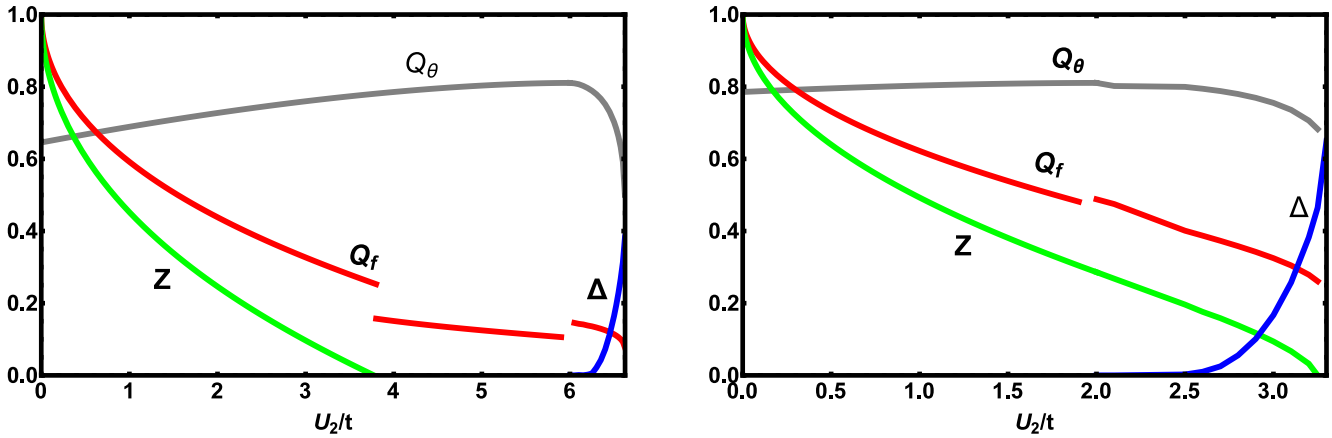

FIG. 2: (color online) Zero temperature physical properties as a function of U_2 at $U_0 = 6t$ (Left Panel) and at $U_0 = 2t$ (Right Panel). *Left*: The quasiparticle weight Z (green line) continuously and monotonically decreases from unity to zero showing metal to Mott-insulator transition at $U_2 \approx 3.8t$. For $3.8t \leq U_2 \leq 6t$, both quasiparticle weight and the pairing order parameter remain zero showing Mott-insulating phase. For $U_2 > 6t$, the singlet pairing order parameter Δ (blue line) becomes finite, indicating Mott-insulator to superconductor transition. *Right*: Only the metallic phase exists for low values of U_2 showing non-zero Z and zero Δ. For $2t \leq U_2 \leq 3.3t$, the existence of Z-SC phase is evident as both Z and Δ have non-zero values. Notice for both cases, while Q_θ (gray line) is continuous at each phase boundary, Q_f shows discontinuities. For clarity, the pairing order parameter Δ has been increased by factor five in these figures.

to that of the metallic phase. In the SC phase, the rotors give non-zero charge gap $\delta_c = 2\sqrt{U(\lambda - \eta t Q_\theta)}$, as similar to that of the Mott-insulating phase.

Here in the present work, we have decoupled the rotor and spinon part of the Hamiltonian using a mean-field theory. We do not expect the inclusion of fluctuation to alter the qualitative features. However the physical observable can slightly be different once the direct coupling between the rotors and spinons are restored. Fluctuations can easily be included by going beyond the saddle point approximation. From the transition from metal phase or Z-SC phase, the quasiparticle weight vanishes, however the effective spinon hopping tQ_f is finite. As a result, the effective mass does not diverge at these transitions. We believe this is an artifact of our mean-field theory. In the presence of fluctuation of a gauge field, the zero-sound Goldstone mode will combine with a gauge boson through Anderson-Higgs mechanism. We believe that this would recover our metal phase as a proper Fermi liquid phase with a diverging Fermi liquid mass [52]. In addition to the mean-field approximation, we treated our constraint globally and assumed all parameters are bond

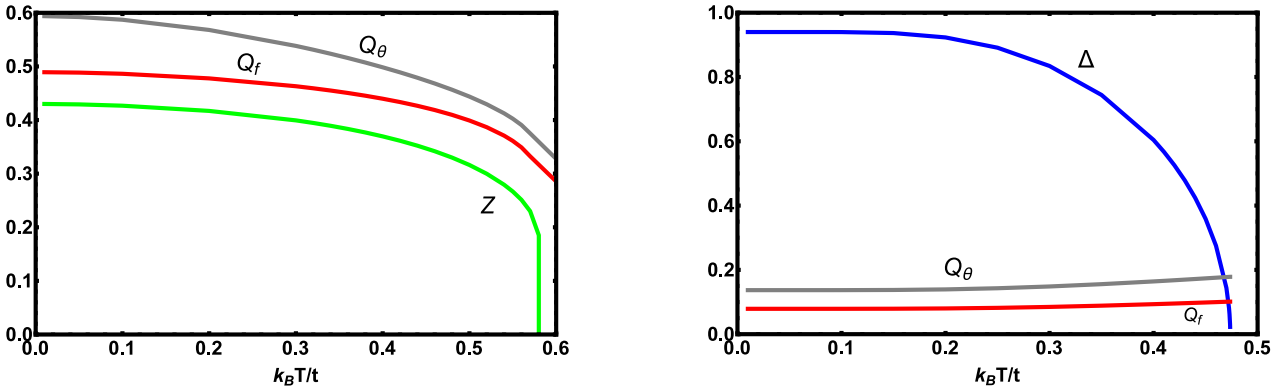

FIG. 3: (color online) Finite temperature properties of the Z-SC phase (right) and metallic phase (left) of fermions in three dimensional cubic lattice. The left graph shows the quasiparticle weight (Z) as a function of temperature k_BT/t in the metallic phase. The interaction parameters were chosen as $U_2 = 2t$ and $U_0 = 4t$. The quasiparticle weight (green line) monotonically decreases from ground state metallic phase to Mott-insulating phase at $k_BT/t \approx 0.58t$. Notice that the finite temperature metal-insulator transition is first order showing a discontinuity of Z at the transition. At the transition, both Q_θ and Q_f finite and continuous. The right graph shows the superconducting order parameter (Δ) as a function of temperature k_BT/t in the Z-SC phase close to the Z-SC-SC boundary. The interaction parameters were chosen as $U_2 = 1.5t$ and $U_0 = 0.5t$, While Δ continuously decreases (blue line) from a finite value to zero showing second order thermal phase transition, both Q_f and Q_θ values remain almost constant as a function of temperature.

independent. We do not expect these approximations to change any qualitative features, specially for the square and cubic lattices discussed.

On the experimental side, spin-3/2 alkaline-earth atoms, such as ^{135}Ba and ^{137}Ba can be promising candidates for observing the Z-SC novel emerging phase. Even though the full spectrum of scattering lengths are not available yet, it is predicted that both scattering lengths a_0 and a_2 should have similar values [38, 53]. Therefore, we believe experiments can find a suitable parameter window in the phase diagram to observe the Z-SC phase even if scattering lengths cannot be independently tuned. On the other hand, the pairing phenomena and the emerging novel phase discussed here is much more general concept associates with many body systems. Thus, the Z-SC phase must exist in other many body systems where competing interactions are taking place. One such example is spin-3/2 rare-earth based half-Heusler semimetals [54–59]. Another promising electronic compound is rubidium doped fullerids [60]. Though on-site interaction is repulsive, the effective negative Hunds coupling due to phonon screening effect can leads to a pairing of electrons [61, 62]. Indeed, a recent experiment finds a novel phase termed by Jahn-Teller metal in rubidium doped fullerids [60]. Perhaps, the superconducting critical temperature enhancement close to the tri-critical point of paramagnetic metal, paramagnetic insulator, and superconducting phases indicates the Z-SC phase in this rubidium doped fullerids compound [63].

The superfluid density, charge gap, and quasiparticle weight all can be measured with currently available experimental techniques in cold gas experiments. For example, the momentum distribution of the atoms can be probed by the absorption imaging after a period of ballistic expansion or in trap in-situ imaging [64]. The charge gap can be detected by measuring the fraction of atoms residing in a lattice site [65]. The superconducting order can be probed by the momentum-resolved Bragg spectroscopy [66]. In addition, the periodic forcing can also be used as a detecting and manipulating tool for many-body states of ultra-cold atomic quantum gases in optical lattices [67]. Though we neglected it in this study, the underlying harmonic trapping potential present in all cold gas experiments causes the density to monotonically vary across the lattice. As a result, the edge of the trap will not be at half filling. As the metallic phase is favorable over the Mott-insulating phase away from half filling, we expect metallic phase to dominate over Mott-insulating phase in the phase diagram.

In conclusion, we have studied the competition of emerging phases of spin-3/2 fermions subjected to a periodic lattice potential using a slave rotor approach. In addition to the well known Fermi liquid metallic phase, Mott-insulating phase, and singlet pairing superconducting phase, we discovered the possibility of having novel emerging superconducting phase due the competing interactions. The novel superconducting phase is characterized by the global U(1) broken symmetries with respect to both roton and spinon fields. Experimentally, this novel phase can be differentiated from regular superconducting phase by its non-zero quasiparticle weight. Further, we have calculated properties of these phases for fermions in both two dimensional square lattice and three dimensional cubic lattice geometries at zero and

finite temperatures.

X. X. ACKNOWLEDGMENTS

We acknowledge the support of Augusta University, the hospitality of ITAMP at the Harvard-Smithsonian Center for Astrophysics and KITP at UC-Santa Barbara. The initial part of the research was undertaken at ITAMP and ITAMP is supported by a grant from the National Science Foundation to Harvard University and the Smithsonian Astrophysical Observatory. The research was completed at KITP, where the research was supported in part by the National Science Foundation under Grant No. NSF PHY11-25915.

[1] M. Lewenstein, A. Sanpera, V. Ahufinger, B. Damski, A. Sen(De) and U. Sen, Advances in Physics **56** (2), 243 (2007).
[2] For an example, Quantum Gas Experiments: Exploring Many-Body States (Cold Atoms, Vol 3), Paivi Torma and Klaus Sengstock, Imperial College Press, London (November 5, 2014).
[3] I. Bloch, Nature Physics **1**, 23, (2005).
[4] Markus Greiner, Olaf Mandel, Tilman Esslinger, Theodor W. Hansch and Immanuel Bloch, Nature **415**, 39 (2002).
[5] Robert Jordens, Niels Strohmaier, Kenneth Gunter, Henning Moritz and Tilman Esslinger, Nature **455**, 204 (2008).
[6] U. Schneider, L. Hackermller, S. Will, Th. Best, I. Bloch, T. A. Costi, R. W. Helmes, D. Rasch, and A. Rosch, Science **322**, 1520 (2008).
[7] R. Jordens, L. Tarruell, D. Greif, T. Uehlinger, N. Strohmaier, H. Moritz, T. Esslinger, L. De Leo, C. Kollath, A. Georges, V. Scarola, L. Pollet, E. Burovski, E. Kozik, and M. Troyer, Phys. Rev. Lett. **104**, 180401 (2010).
[8] L. Hackermuller, U. Schneider, M. Moreno-Cardoner, T. Kitagawa, T. Best, S. Will E. Demler, E. Altman, I. Bloch, B. Paredes, Science **327**, 1621 (2010).
[9] T. B. Ottenstein, T. Lompe, M. Kohnen, A. N. Wenz, and S. Jochim, Phys. Rev. Lett. **101**, 203202 (2008).
[10] J. H. Huckans, J. R. Williams, E. L. Hazlett, R. W. Stites, and K. M. OHara, Phys. Rev. Lett. **102**, 165302 (2009).
[11] A. N. Wenz, T. Lompe, T. B. Ottenstein, F. Serwane, G. Zurn, and S. Jochim, Phys. Rev. A **80**, 040702(R) (2009).
[12] G. Modugno, F. Ferlaino, R. Heidemann, G. Roati, and M. Inguscio, Phys. Rev. A **68**, 011601(R) (2003).
[13] L.-W. He, C. E. Burkhardt, M. Ciocca, J. J. Leventhal, and S. T. Manson, Phys. Rev. Lett. **67**, 2131 (1991).
[14] T. Fukuhara, Y. Takasu, M. Kumakura, and Y. Takahashi, Phys. Rev. Lett. **98**, 030401 (2007).
[15] S. K. Yip and T. L. Ho, Phys. Rev. A **59**, 4653 (1999)
[16] C. Wu, J. P. Hu and S. C. Zhang, Phys. Rev. Lett. **91**, 186402 (2003).
[17] E. Szirmai, G. Barcza, J. Sólyom, and ö. Legeza, Phys. Rev. A **95**, 013610 (2017).
[18] Wang Yang, Yi Li, and Congjun Wu, Phys. Rev. Lett. **117**, 075301 (2016).
[19] D. Jakab, E. Szirmai, M. Lewenstein, and G. Szirmai, Phys. Rev. B **93**, 064434 (2016).
[20] J. J. Hernández-Sarria, K. Rodŕguez, J Supercond Nov Magn (2015) 28:28092813
[21] S. Capponi, G. Roux, P. Azaria, E. Boulat, and P. Lecheminant, Phys. Rev. B **75**, 100503(R) (2007).
[22] Hong-Hao Tu, Guang-Ming Zhang, and Lu Yu, Phys. Rev. B 76, 014438 (2007).
[23] R. W. Cherng, G. Refael, and E. Demler, Phys. Rev. Lett. **99**, 130406 (2007).
[24] Cenke Xu, Phys. Rev. B **78**, 054432 (2008).
[25] C. WU, J. HU, and S-C. ZHANG, Int. J. Mod. Phys. B **24**, 311 (2010).
[26] Yusuke Nishida and Dam T. Son, Phys. Rev. A **82**, 043606 (2010).
[27] C. Wu, Mod. Phys. Lett. B, **20**, 1707 (2006).
[28] S. Chen, Phys. Rev. B **72**, 214428 (2005).
[29] P. Schlottmann, J. Phys: Cond. Matt. 6, 1359 (1994).
[30] H. Kamei and K. Miyake, J. Phys. Soc. Jpn. **74**, 1911 (2005).
[31] C. Wu, Phys. Rev. Lett. **95**, 155115 (2005).
[32] D. Lee, Phys. Rev. A **73**, 63204 (2006).
[33] C. Honerkamp and W. Hofstetter, Phys. Rev. Lett. **92**, 170403 (2004).
[34] A. Rapp, G. Zarand, C. Honerkamp and W. Hofstetter, Phys. Rev. Lett. **98**, 160405 (2007).
[35] S. Florens and A. Georges, Phys. Rev. B **66**, 165111 (2002).
[36] G. Roux, S. Capponi, P. Lecheminant, and P. Azaria, Eur. Phys. J. B **68**, 293308 (2009).
[37] C. Wu, J.-P. Hu, S.-C. Zhang, Phys. Rev. Lett. **91**, 186402 (2003).
[38] C. Wu, J. Hu, and S-C. Zhang, Int. J. Mod. Phys. B **24**, 311 (2010).
[39] I. Bloch, J. Dalibard, and W. Zwerger, Many-body physics with ultracold gases, Rev. Mod. Phys. **80**, 885 (2008).
[40] G. Kotliar and A. E. Ruckenstein, Phys. Rev. Lett. **57**, 1362 (1986).
[41] R. L. Stratonovich, Doklady Akad. Nauk SSSR **115** 1097, (1957); [translation: Soviet Phys.-Doklady **2**, 416 (1958)].
[42] J. Jedrak, J. Kaczmarczyk, and J. Spalek, preprint, (2010), http://arxiv.org/abs/1008.0021.
[43] M. C. Gutzwiller, Phys. Rev. **137**, A1726 (1965).
[44] D. Vollhardt, Rev. Mod. Phys. **56**, 99 (1984).
[45] G. Wang, M. O. Goerbig, C. Miniatura and B. Gŕemaud, EPL, **95** (2011) 47013.
[46] Sung-Sik Lee and Patrick A. Lee, Phys. Rev. Lett. **95**, 036403 (2005).
[47] Stephan Rachel and Karyn Le Hur, Phys. Rev. B **82**, 075106 (2010).
[48] Serge Florens, Priyanka Mohan, C. Janani, T. Gupta and R. Narayanan, EPL, **103** (2013) 17002
[49] Ki-Seok Kim, Jung Hoon Han, pre-print arXiv:cond-

mat/0605266.
[50] E. Zhao and A. Paramekanti, Phys. Rev. B **76**, 195101 (2007).
[51] Serge Florens and Antoine Georges, Phys. Rev. B **70**, 035114 (2004).
[52] W. Witczak-Krempa, P. Ghaemi, T. Senthil, and Yong Baek Kim, Phys. Rev. B **86**, 245102 (2012).
[53] M. Machholm, P. S. Julienne, and K. A. Suominen, Phys. Rev. A **64**, 33405 (2001).
[54] P. M. R. Brydon, Limin Wang, M. Weinert, D.F. Agterberg, Phys. Rev. Lett. **116**, 177001 (2016).
[55] H. Kim et at., arXiv:1603.03375.
[56] C. Timm, A. P. Schnyder, D. F. Agterberg, P. M. R. Brydon Phys. Rev. B **96**, 094526 (2017).
[57] Jorn W. F. Venderbos, Lucile Savary, Jonathan Ruhman, Patrick A. Lee, Liang Fu, arXiv:1709.04487.
[58] Lucile Savary, Jonathan Ruhman, Jrn W. F. Venderbos, Liang Fu, Patrick A. Lee, arXiv:1707.03831.
[59] Bitan Roy, Sayed Ali Akbar Ghorashi, Matthew S. Foster, Andriy H. Nevidomskyy, arXiv:1708.07825.
[60] R. H. Zadik *et al.* ,Sci. Adv. **1**, e1500059 (2015).
[61] M. Fabrizio and E. Tosatti, Phys. Rev. B **55**, 13465 (1997).
[62] S. Hoshino, P. Werner, Phys. Rev. Lett. **118**, 177002 (2017).
[63] Y. Nomura *et al.* Sci. Adv. **1**, e1500568 (2015).
[64] U. Schneider, L. Hackermller, S. Will, Th. Best, I. Bloch, T. A. Costi, R. W. Helmes, D. Rasch, A. Rosch, Science, **322**, 1520 (2008).
[65] Robert Jördens, Niels Strohmaier, Kenneth Günter, Henning Moritz, and Tilman Esslinger, Nature **455**, 204-207 (2008).
[66] Philipp T. Ernst, Sören Götze, Jasper S. Krauser, Karsten Pyka, Dirk-Sören Lühmann, Daniela Pfannkuche, and Klaus Sengstock, Nature Physics **6**, 56 - 61 (2010).
[67] André Eckardt, Rev. Mod. Phys. **89**, 011004 (2017).